Available online at www.sciencedirect.com
ScienceDirect
Carbohydrate Research 341 (2006) 2575–2580
Carbohydrate RESEARCH

B3LYP/6-311++G** study of structure and spin–spin coupling constant in methyl 2-*O*-sulfo-α-L-iduronate

Miloš Hricovíni*

Institute of Chemistry, Slovak Academy of Sciences, 845 38 Bratislava, Slovakia

Received 26 April 2006; received in revised form 10 July 2006; accepted 18 July 2006
Available online 23 August 2006

Abstract—Structures of three most stable conformers ($^1C_4$, $^4C_1$, $^2S_0$) of methyl 2-*O*-sulfo-α-L-iduronate monosodium salt have been analyzed by DFT using the B3LYP/6-311++G** method. The optimized geometries confirmed the influence of both 2-*O*-sulfate and carboxylate groups upon the pyranose ring geometry. The computed energies showed that the chair $^1C_4$ form is the most stable one. Time-averaged DFT-calculated proton–proton and proton–carbon spin–spin coupling constants agree with the experimental data and indicate that only two chair forms contribute to the conformational equilibrium of methyl 2-*O*-sulfo-α-L-iduronate monosodium salt. The influence of the charged groups upon the magnitudes of spin–spin coupling constants is also discussed.

Keywords: Methyl 2-*O*-sulfo-α-L-iduronate; Conformation; Quantum mechanical calculations; Coupling constants

1. Introduction

Glycosaminoglycans (GAGs) are heterogeneous polysaccharides made up by alternating uronic acid (glucuronic acid or iduronic acid) and hexosamine (2-amino-2-deoxy-D-glucose, 2-amino-2-deoxy-D-galactose).[1,2] These residues can be substituted to various degree by O- or N-sulfated (O–SO_3^- or N–SO_3^-) groups.[3] Conformations, dynamics and intermolecular interactions of GAGs have been thoroughly studied aimed at detailed understanding of their interactions with proteins.[4–7] Experimental and theoretical studies revealed that the 2-*O*-sulfo-α-L-iduronate residue has unique conformational properties in oligo- and polysaccharides.[8–11] 3D structure of this residue has been the subject of particular interest as this residue plays one of the key roles in intermolecular interactions of GAGs with proteins.[1,4–7,12] NMR and theoretical analyses showed that three forms, $^1C_4$, $^4C_1$ and $^2S_0$, are predominantly present in conformational equilibrium of the residue and that populations of these conformers depend upon the structure of neighbouring units, type of counterions and concentration.[2,7,11,13–15] Molecular mechanics, dynamics and quantum chemical calculations, together with the analysis of NMR spin–spin coupling constants and NOEs, enabled estimation of conformer populations in different oligo- and polysaccharides as well as the geometry of these residues. Molecular mechanics[16] and dynamics calculations[17] showed that the three forms of methyl 2-*O*-sulfo-α-L-iduronate have comparable energies though the energy differences among the conformers differed in these studies. Continuous graphical approach analyzing the pyranose ring flexibility indicated relatively complex conformational equilibria of the iduronate residues in GAGs.[18]

This paper reports results from DFT calculations of three conformers of methyl 2-*O*-sulfo-α-L-iduronate monosodium salt (IdoA2SNa) using the B3LYP/6-311++G** method. High level basis set, including diffuse functions, is important when dealing with saccharides bearing sulfate and carboxylate groups. DFT calculations at the B3LYP/6-311++G** level of theory gave recently reliable energies and geometries for several carbohydrates.[19–23] Well-refined structures are essential for calculations of other theoretical data, such as NMR parameters. Previous calculations on structurally

* Tel.: +421 2 59410323; fax: +421 2 59410222; e-mail: hricovini@savba.sk

0008-6215/$ - see front matter © 2006 Elsevier Ltd. All rights reserved.
doi:10.1016/j.carres.2006.07.010

similar compounds,[24,25] obtained using the B3LYP/6-31+G* and B3LYP/6-31+G* basis sets, enabled calculations of geometries, energies and thermochemical parameters. Ionizations of sodium salts of variously substituted monosaccharides were associated with conformational rearrangements of the ionic species. These rearrangements caused an additional energetic stabilization of anionic groups. Calculations also showed that geometrical parameters in water do not considerably differ from those obtained for isolated state. Computed geometries were not comparable in several parameters with those previously derived by molecular mechanics or dynamics and prompted us to extend these calculations using the B3LYP/6-311++G** method. In addition, DFT-based NMR spin–spin coupling constants were compared with experimental values measured in the same compound.

2. Computational methodology

The geometries of three IdoA2SNa conformers ($^1C_4$, $^4C_1$ and $^2S_0$, Scheme 1) have been completely optimized with the JAGUAR program[26] using density functional theory (DFT)[27] with Lee–Young–Parr (B3LYP)[28] correlation functional and the 6-311++G** basis set. The starting geometries ($^1C_4$, $^4C_1$ and $^2S_0$ conformers) for optimization were obtained by B3LYP/6-31+G* method.[29] Hybrid functionals with the Slater local functional/Becke88 non-local gradient correlation[30] and Vosko–Wilk–Nusair local functionals[31] were used. Geometry optimizations were obtained with the gradient optimization routine, the convergence criteria were set to 1.10^{-5}. NMR proton–proton and proton–carbon spin–spin coupling constants were computed with the GAUSSIAN03 program[32] at the B3LYP/DGDZVP level of theory.[33] Solvation energies were obtained by both self-consistent reaction field method[34] implemented in the JAGUAR program and by the polarizable conductor calculation model (CPCM)[35] implemented in the GAUSSIAN03 program.

3. Results and discussion

3.1. Geometry

Selected optimized bond lengths for three conformers, $^1C_4$, $^4C_1$ and $^2S_0$, of IdoA2SNa are given in Table 1. Inspections of the data indicate that the bond lengths vary with the form of the ring and are comparable with the experimental data (last column in Table 1) of the structurally-related compounds.[36–38] The largest differences among three different forms are, as expected, in the C-1–O-1 (0.068 Å), C-1–O-5 (0.043 Å) and C-5–O-5 (0.022 Å) bond lengths. The inter-atomic distances in the 2-*O*-sulfate group reveal that both S-1–O-9 and S-1–O-10 are longer (1.481–1.497 Å) than the S-1–O-8 distance (1.449–1.453 Å) in both the $^1C_4$ and the $^4C_1$ conformers. The bond lengths and atomic charges on both O-9 and O-10 (Table 2) suggest the resonance bond character of the S-1–O-9 and S-1–O-10 linkages whereas the S-1–O-8 bond is double bond. In the $^2S_0$ conformer, however, O-8 and O-9 oxygens are more negatively charged (Table 2) and the S-1–O-10 distance is shorter (1.447 Å), the latter again in agreement with the double bond character. The shorter S-1–O-10 distance, rather than the S-1–O-8 bond in the chair forms, is obviously due to the different coordination of the Na-1 ion ($-SO_3^- \cdots Na^+ \cdots$O-1) in the skewed conformer with respect to both chair forms (Scheme 1). The evidence of the two longer S–O bonds and one double bond in the $-SO_3^-$ group is in agreement with the published crystal data of N-sulfated glucosamine[37] where the measured S–O distance of the double bond was 1.446 Å.

As mentioned, the coordination of the Na-1^+ ion varies within the three conformers. In the $^2S_0$ form, sodium ion is located between O-8 and O-9 and the anomeric O-1 (Scheme 1). Unlike this, Na-1^+ is coordinated with –O-3 in the $^4C_1$ or with –O-4 in the $^1C_4$ chair form. The distances between Na-1^+ ions and adjacent oxygens are comparable with each other in all three forms and is similar to experimentally observed sodium-to-oxygen

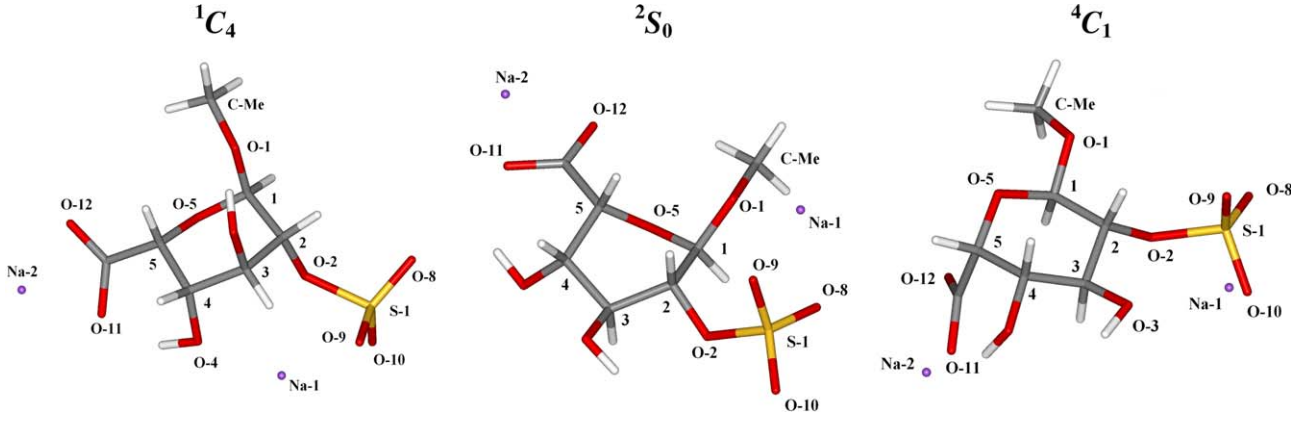

Scheme 1. Schematic representation of three conformations of methyl 2-*O*-sulfo-α-L-iduronate monosodium salt.

Table 1. Selected optimized (B3LYP/6-311++G**) bond lengths (in Å) for three conformers, $^1C_4$, $^4C_1$ and $^2S_0$ in IdoA2SNa

Bond	$^1C_4$	$^2S_0$	$^4C_1$	Exp.[a] $^1C_4$
C1–C2	1.534	1.542	1.544	1.515
C2–C3	1.544	1.539	1.529	1.529
C3–C4	1.544	1.534	1.530	1.532
C4–C5	1.535	1.542	1.539	1.535
C5–O5	1.437	1.434	1.412	1.406
C1–O5	1.417	1.396	1.439	1.425
C1–O1	1.414	1.447	1.379	1.381
C5–C6	1.540	1.536	1.546	1.516
C2–O2	1.429	1.433	1.431	
S1–O2	1.734	1.684	1.684	
S1–O8	1.453	1.494	1.449	1.446[b]
S1–O9	1.485	1.498	1.497	1.466[b]
S1–O10	1.481	1.447	1.494	1.457[b]
S1–Na1	2.670	2.764	2.749	
O8–Na1	2.545	2.269	2.292	
O9–Na1	2.420	2.277	2.270	
O1–Na1		2.312		
O4–Na1	2.248			
O3–Na1			2.272	
C6–O11	1.281	1.272	1.280	
C6–O12	1.251	1.256	1.251	
O11–Na2	2.237	2.227	2.241	
O12–Na2	2.228	2.231	2.230	

Experimental values of structurally-related compounds are in the last column.

[a] Taken from Ref. 36.

[b] Taken from Ref. 37.

Table 2. Atomic charges from Mulliken population analysis for selected atoms for three conformers, $^1C_4$, $^4C_1$ and $^2S_0$ in IdoA2SNa

Atom	$^1C_4$	$^2S_0$	$^4C_1$
C1	0.182	0.226	0.150
C2	0.083	0.027	0.041
C3	0.019	0.033	0.082
C4	0.063	0.013	0.018
C5	0.084	0.045	−0.040
C6	0.295	0.282	0.295
C_{Me}	−0.156	−0.145	−0.157
O1	−0.446	−0.571	−0.334
O2	−0.610	−0.466	−0.449
O3	−0.389	−0.378	−0.590
O4	−0.585	−0.392	−0.465
O5	−0.354	−0.339	−0.329
O8	−0.471	−0.600	−0.466
O9	−0.542	−0.628	−0.627
O10	−0.537	−0.455	−0.584
O11	−0.619	−0.569	−0.605
O12	−0.445	−0.509	−0.446
S1	1.122	1.137	1.144
Na1	0.802	0.807	0.823
Na2	0.807	0.797	0.817

distances.[37] It should be noted that the starting positions (before geometry optimization) of Na-1$^+$ ions were the same in both $^1C_4$ and the $^2S_0$ forms (Na-1$^+$ was located among O-8, O-9 and the anomeric O-1). Sodium ion changed considerably its position during optimization in the $^1C_4$ chair form (coordination with O-1 before optimization, coordination with O-4 in the minimized structure) whereas Na-1$^+$ remained close to the anomeric O-1 in the $^2S_0$ form. The inter-atomic distances in the carboxylate group are nearly the same in all the three conformations. The differences are, however, between the C-6–O-11 and C-6–O-12 bond lengths with the first one being longer due to the intra-molecular hydrogen bond with the HO-4. This hydrogen bond was present in all three forms of **1**. The differences in the C-6–O-11 and C-6–O-12 bond lengths were observed also in the methylated carboxyl group in the crystal structure of tri-O-acetylated derivative of methyl iduronate.[36] Nevertheless, longer C-6–O-11 distance in the latter case was due to the presence of the methyl group rather than the hydrogen bond.

Atomic charges at oxygen atoms, predominantly on O-1, O-3 and O-4 differed with each other according to coordinations of Na-1$^+$ in three conformers of **1** (Table 2). The charges of these oxygens were comparably for those atoms that were involved in coordination with Na-1$^+$, thus O-4 in the $^1C_4$ form (−0.585), O-1 in the $^2S_0$ form (−0.571) and O-3 in the $^4C_1$ conformer (−0.590) (Table 2). The charges at non-coordinated atoms were considerable lower (−0.334 up to −0.465). Similarly in the sulfate group, oxygens coordinated with sodium (e.g., O-9 and O-10 for chair forms) had higher charges than those involved in double bonds (e.g., O-8 for chair forms). The differences in atomic charges were obtained also for O-11 and O-12, O-11 being more negatively charged, and in agreement with the observed intra-molecular hydrogen bond.

Variations in other geometrical parameters, bond angles and torsions angles (Tables 3 and 4), were also largest in the anomeric part (e.g., O-5–C-1–O-1, O-1–C-1–C-2, C-1–O-1–C_{Me} bond angles) of the molecule. The values of torsion angles indicate that both sulfate and carboxylate groups influence the ring geometry of this monosaccharide. Comparison with the crystal structure of tri-O-acetylated derivative points out of the difference in ring puckering in the two molecules. As a result, the values of three-bond proton–proton coupling

Table 3. Selected optimized and experimental bond angles for IdoA2SNa (in °)

Bond angle	$^1C_4$	$^2S_0$	$^4C_1$	Exp.[a] $^1C_4$
O5–C1–C2	112.2	112.3	112.5	111.1(4)
O5–C1–O1	111.9	109.8	107.4	109.9(3)
O1–C1–C2	106.9	109.0	107.6	109.9(4)
C1–C2–C3	111.0	110.6	110.8	111.1(4)
C1–O1–C_{Me}	114.5	112.1	114.6	
S1–O2–C2	118.7	120.0	121.5	118.1(6)[b]

Experimental values of structurally-related compounds are in the last column.

[a] Taken from Ref. 36.

[b] Taken from Ref. 37.

Table 4. Selected optimized and experimental torsion angles for IdoA2SNa (in °)

Torsion angles	$^1C_4$	$^2S_0$	$^4C_1$	Exp.[a] $^1C_4$
O5–C1–C2–C3	−52.0	23.9	45.9	−52.9
C6–C5–O5–C1	175.0	158.9	−65.3	170.3
O5–C1–C2–O2	69.6	140.4	165.6	66.6
O5–C1–C2–C_{Me}	−61.6	−82.3	−174.8	
C1–C2–C3–C4	47.9	−56.5	−46.8	42.8
C2–C3–C4–C5	−48.1	25.1	54.3	−42.8
C3–C4–C5–O5	52.6	35.4	−59.7	54.2
C2–C1–O1–C_{Me}	170.7	−178.5	161.3	−162.1
C1–C2–O2–S1	147.6	85.0	141.8	
H1–C1–O5–C5	178.0	160.2	64.9	
H1–C1–O1–C_{Me}	50.4	61.0	41.3	
H5–C5–O5–C1	60.6	45.4	178.4	
H1–C1–C2–C3	−168.2	−94.8	−74.9	
H2–C2–C3–C4	167.9	65.5	74.1	
H3–C3–C4–C5	−167.5	−93.2	−65.8	
H3–C3–C2–C1	168.6	61.2	74.1	
H1–C1–C2–H2	71.6	143.4	162.8	55.0
H2–C2–C3–H3	−71.2	−176.8	−165.0	−73.0
H3–C3–C4–H4	74.6	149.3	177.5	72.0
H4–C4–C5–H5	48.8	33.9	−56.5	56.0

Experimental values of structurally-related tri-*O*-acetyl derivative are in the last column.
[a] Taken from Ref. 36.

constants differ from each other in these two compounds.[8,36]

Computed relative, zero-point vibrational (ZPVE), corrected relative energies based on the B3LYP/6311++G** geometry optimization of $^1C_4$, $^4C_1$ and $^2S_0$ conformers and their abundances are given in Table 5. The energy values indicate that the $^1C_4$ conformer is the most stable one and that the $^2S_0$ form has the highest relative energy. Significant populations of both $^1C_4$ and $^4C_1$ forms in conformational equilibrium have been obtained in previous molecular mechanics study.[16] However, the energy difference among all three conformers (including the $^2S_0$ form) was smaller indicating higher abundance of the $^4C_1$ and the $^2S_0$ forms with respect to the present data. On the other hand, MD simulations[17] revealed considerable pseudorotation among all three forms of the iduronate ring. NMR spin–spin coupling constants, based on the Haasnoot et al. parametrization,[39] gave higher values than experimentally observed. Better agreement between the experimental and computed data were obtained when considering only the $^1C_4$ and $^2S_0$ conformers.[8]

Table 5. Calculated relative (ΔE), zero-point vibrational (ZPVE) and corrected relative (ΔE_{corr}) energies (values in kcal/mol) based on the B3LYP/6311++G** geometry optimization of the three most stable conformers of IdoA2SNa

	$^1C_4$	$^2S_0$	$^4C_1$
ΔE	0[a]	7.690	2.775
ZPVE	121.492	121.186	121.396
ΔE_{corr}	0	7.384	2.679
Abundance	98.9	0	1.1
ΔE[b]	2.666	4.623	0
ΔE[c]	1.154	2.871	0

Relative energies obtained by CPCM method and reaction field method are listed in last two rows. The abundances of conformers in isolated state are also given.
[a] Energy: −1748.2210886.
[b] Reaction field method.[34]
[c] CPCM method.[35]

Geometry optimizations of all three conformers in aqueous solutions using both the reaction-field method[34] and the CPCM method[35] yielded energies that did not correspond to the experimental evidence. The most stable conformer was $^4C_1$ (in both methods), and the $^1C_4$ form had more than 1 kcal/mol higher energy (Table 5). In the first method of solvent calculations, higher energy of the $^1C_4$ form was due to the difference in the solvent reorganization energy (7.118 kcal/mol; data not shown) that was higher for the $^1C_4$ form than for the other chair form. Similarly, this energy contribution was higher (4.915 kcal/mol) also for the $^2S_0$ conformer compared to the $^4C_1$ form. As the cavity terms were comparable for all three forms, the data suggested that the reorganization energy contribution to the solvent energy is the main source of discrepancies in total energies. Similarly in the CPCM model, the cavity terms (as in the previous method) and repulsion energy were comparable for both forms. A small difference was obtained for the dispersion energy that was lower (0.37 kcal/mol) for the $^4C_1$ conformer compared to the $^1C_4$ form. As expected, the polarizable solute–solvent energy contribution, unlike non-electrostatic terms, was the main cause of the solvent energy differences. The computed difference in this electrostatic term was 13.7 kcal/mol in favour of the $^4C_1$ conformer. The above data thus show that dielectric continuum approaches failed to describe quantitatively solvent energies of three IdoA2SNa conformers. Considerably charged molecules, such as heparin-like saccharides, seem to require more precise solvent treatment in order to describe fine conformer distribution of these compounds in aqueous solutions.

3.2. NMR spin–spin coupling constants

Computed three-bond proton–proton coupling constants ($^3J_{H–H}$) in IdoA2SNa are given in Table 6. Experimental values, measured in the same compound,[8] are listed together with the values collected in structurally-related acetyl derivative.[36] The computed $^3J_{H–H}$ values in the $^1C_4$ form agree well with the experimental data; small discrepancies are in $^3J_{H-2,H-3}$ and $^3J_{H-3,H-4}$ values (0.34 and 0.32 Hz, respectively). The time-averaged values, taking into account the contribution (1 %) of the $^4C_1$ chair form to the conformational equilibrium, are thus in excellent agreement with the experiment and confirm that the major conformer (99%) is the $^1C_4$ one whereas the population of the other chair form is

Table 6. Computed, time-averaged (fifth column) and experimental (sixth column) three-bond proton–proton coupling constants (values in hertz) for three conformers, $^1C_4$, $^4C_1$ and $^2S_0$ in IdoA2SNa

	$^1C_4$	$^2S_0$	$^4C_1$	$^1C_4$:$^4C_1$ 99:1	Exp.[8]	Exp.[36] tri-*O*-acetyl derivative
H1–H2	1.67	4.76	7.31	1.73	1.76	2.2
H2–H3	3.00	10.53	9.01	3.06	3.34	4.5
H3–H4	3.12	4.49	10.22	3.19	3.44	4.4
H4–H5	2.30	4.11	6.53	2.34	2.22	2.8

Experimental values of structurally-related tri-*O*-acetyl derivative are in the last column.

very small. Previous analysis, based on molecular mechanics[8] and the empirical parametrization[39] of $^3J_{H–H}$, suggested that the conformational equilibrium consists of the $^1C_4$ and $^2S_0$ forms in a ratio of about 90:10.[8] The largest deviations were obtained in $^3J_{H\text{-}1,H\text{-}2}$ and $^3J_{H\text{-}4,H\text{-}5}$ (nearly 1 Hz). Both molecular mechanics-derived geometry and empirical parametrization could cause larger discrepancies between the theoretical and experimental data and led to the equilibrium of the $^1C_4$ chair and skew $^2S_0$ conformers.

The computed data also show that atom electronegativities and the presence of charged groups considerably affect the values of coupling constants. $^3J_{H\text{-}4,H\text{-}5}$ coupling constant is a good example of such an influence. Its value (2.30 Hz) is smaller than the $^3J_{H\text{-}3–H\text{-}4}$ (3.12 Hz) in the $^1C_4$ conformer. Nearly 30° difference in the torsion angles (Table 4) would suggest the opposite trend of the coupling constants magnitudes as the angle between the H-4 and H-5 atoms is smaller (48.8°) than that for the H-3–H-4 atoms (74.6°). However, the computed Fermi term is 2.84 Hz for the $^3J_{H\text{-}3,H\text{-}4}$ and is larger than that for the $^3J_{H\text{-}4,H\text{-}5}$ coupling constant (1.58 Hz) (Table 7). The same is valid for paramagnetic and diamagnetic contributions, though they partially cancel each other due to their opposite signs. Thus, the resulting scalar coupling constant between H-4 and H-5 atoms is smaller than one would expect considering exclusively the stereochemical arrangement. Similarly, the $^3J_{H\text{-}2,H\text{-}3}$ value is larger than that of $^3J_{H\text{-}1,H\text{-}2}$ whereas the corresponding torsions angles (−71.2° and 71.6°) would suggest comparable coupling constants. The influence of the 2-*O*-sulfate group is remarkable upon both $^3J_{H\text{-}1,H\text{-}2}$ and $^3J_{H\text{-}2,H\text{-}3}$ values. It is noteworthy, however that there is a good agreement between theory and experiment where all computed values are within the experimental error assuming small contribution (about 1%) of the $^4C_1$ chair form to the conformational equilibrium.

Selected computed three-bond proton–carbon coupling constants ($^3J_{H–C–C–C}$ and $^3J_{H–C–O–C}$) are listed in Table 8. In general, both types of coupling constants follow the Karplus-type relationship. In some cases, the influences of the stereo-electronic effects are considerable and should be taken into account when interpreting these NMR parameters. This is mainly valid for $^3J_{H–C–O–C}$ coupling constants having oxygen atom in the array of the bonded atoms. The mutual positions and, consequently, the interactions of both O-5 and O-1 lone pairs influence the magnitudes of $^3J_{H–C–O–C}$ values. The interactions of these lone pair with molecular orbitals of the C-1–O-5, C-5–O-5 and C-1–O-1 bonds result not only in geometrical changes (e.g., C-5–O-5 and C-1–O-5 inter-atomic distances in various conformers; Table 1) but also in the electronic structure. Similar effects have been previously observed in magnitudes of $^1J_{C\text{-}H}$ coupling constants in methyl-β-D-xylopyranoside.[40] As a result, some coupling constants have larger values than expected considering only the torsion angle dependence. For example, $^3J_{H\text{-}1,C\text{-}1,O\text{-}5,C\text{-}5}$ is 6.3 Hz (the torsion angle is 178°, Table 4) in the $^1C_4$ conformer whereas 7.6 Hz in the $^2S_0$ conformer (160.2°). Stereo-electronic effects are important in several $^3J_{H–C–C–C}$ coupling constants as well. Their contributions are in general smaller, compared to $^3J_{H–C–O–C}$ coupling constants, but not negligible. More than 0.7 Hz difference between $^3J_{H\text{-}2,C\text{-}2,C\text{-}3,C\text{-}4}$ (3.81 Hz, torsion angle 167.9°) and $^3J_{H\text{-}3,C\text{-}3,C\text{-}2,C\text{-}1}$ (4.52 Hz, torsion angle 168.6°) is large enough for experimental determination.

In summary, very good agreement between the presented theoretical data and the published crystal and NMR evidence demonstrates that DFT calculations

Table 7. Computed individual contributions to the three-bond proton–proton coupling constants (values in hertz) in the $^1C_4$ conformation of IdoA2SNa

	Fermi contact	Spin–dipolar	Paramagnetic spin–orbit	Diamagnetic spin–orbit	Total
H1–H2	1.32	0.05	−0.45	0.74	1.67
H2–H3	2.54	0.06	−0.59	0.97	3.00
H3–H4	2.84	0.06	−0.41	0.63	3.12
H4–H5	1.58	0.14	−1.06	1.63	2.30

Table 8. Selected computed three-bond proton–carbon coupling constants (values in hertz) for three conformers, $^1C_4$, $^4C_1$ and $^2S_0$ in IdoA2SNa

	$^1C_4$	$^2S_0$	$^4C_1$
H1–C1–O5–C5	6.30	7.60	0.45
H1–C1–O1–C_{Me}	3.96	2.28	5.08
H5–C1–O5–C1	1.97	4.53	8.32
H1–C1–C2–C3	2.50	0.00	0.28
H2–C2–C3–C4	3.81	1.93	0.44
H3–C3–C4–C5	4.32	0.07	1.23
H3–C3–C2–C1	4.52	0.98	0.52

at the B3LYP/6-311++G** level of theory can offer reliable results in GAG compounds. The effects of both sulfate and carboxylate groups upon the molecular geometry of IdoA2SNa can be examined by DFT using the high level basis set. The computed energies indicate that the most stable is the $^1C_4$ chair form with the small contribution of the $^4C_1$ form to the conformational equilibrium. This evidence is surprising, as in previous studies, the $^2S_0$ form has been considered in the equilibrium of monosaccharide IdoA2SNa. Such evidence is important and further studies on heparin-oligosaccharides are needed to determine the conformational equilibria in more detail.

Acknowledgement

This research was supported by VEGA grant No. 2/5075/25, APVT grant No. 51-034504 and EU grant No. QLK3-2002-02049.

References

1. Conrad, H. E. *Heparin-Binding Proteins*; Academic Press: San Diego, 1998.
2. Casu, B. *Adv. Carbohydr. Chem. Biochem.* **1985**, *43*, 51–134.
3. *Heparin—Chemical and Biological Properties*; Lane, D. A., Lindahl, U., Eds.; CRC Press: Boca Raton, FL, 1989.
4. Mulloy, B.; Forster, M. J. *Glycobiology* **2000**, *10*, 1147–1156.
5. Casu, B.; Lindahl, U. *Adv. Carbohydr. Chem. Biochem.* **2001**, *57*, 159–208.
6. Capila, I.; Linhardt, R. J. *Angew. Chem., Int. Ed.* **2002**, *41*, 390–412.
7. Hricovíni, M.; Nieto, P. M.; Torri, G. In *NMR Spectroscopy of Glycoconjugates*; Jimenez-Barbero, J., Peters, T., Eds.; Wiley-VCH, 2002; pp 189–229.
8. Ferro, D. R.; Provasoli, A.; Ragazzi, M.; Torri, G.; Casu, B.; Gatti, G.; Jacquinet, J. C.; Sinay, P.; Petitou, M.; Choay, J. *J. Am. Chem. Soc.* **1986**, *108*, 6773–6778.
9. Torri, G.; Casu, B.; Gatti, G.; Petitou, M.; Choay, J.; Jacquinet, J.-C.; Sinay, P. *Biochem. Biophys. Res. Commun.* **1985**, *128*, 134–140.
10. Casu, B.; Petitou, M.; Provasoli, A.; Sinay, P. *Trends Biochem. Sci.* **1988**, *13*, 221–225.
11. Ferro, D. R.; Provasoli, A.; Ragazzi, M.; Casu, B.; Torri, G.; Bossennec, V.; Perly, B.; Sinay, P.; Petitou, M.; Choay, J. *Carbohydr. Res.* **1990**, *195*, 157–167.
12. Sasisekharan, R.; Venkataraman, G. *Curr. Opin. Chem. Biol.* **2000**, *4*, 626–631.
13. Rabenstein, D. L.; Robert, J. M.; Peng, J. *Carbohydr. Res.* **1995**, *278*, 239–256.
14. Chevalier, F.; Lucas, R.; Angulo, J.; Martín-Lomas, M.; Nieto, P. M. *Carbohydr. Res.* **2004**, *339*, 975–983.
15. Whitfield, D. M.; Sarkar, B. *J. Inorg. Biochem.* **1991**, *41*, 157–170.
16. Ragazzi, M.; Ferro, D. R.; Provasoli, A. *J. Comput. Chem.* **1986**, *7*, 105–112.
17. Forster, M. J.; Mulloy, B. *Biopolymers* **1993**, *33*, 575–588.
18. Ernst, S.; Venkataraman, G.; Sasisekharan, V.; Langer, R.; Cooney, C. L.; Sasisekharan, R. *J. Am. Chem. Soc.* **1998**, *120*, 2099–2107.
19. Tvaroška, I.; Carver, J. P. *J. Phys. Chem. B* **1997**, *101*, 2992–2999.
20. Lii, J.-H.; Ma, B.; Allinger, N. L. *J. Comput. Chem.* **1999**, *20*, 1593–1603.
21. Tvaroška, I.; Taravel, F. R.; Utille, J. P.; Carver, J. P. *Carbohydr. Res.* **2002**, *337*, 353–367.
22. Appel, M.; Strati, G.; Willett, J. L.; Momany, F. A. *Carbohydr. Res.* **2004**, *339*, 537–551.
23. Momany, F. A.; Appel, M.; Willett, J. L.; Schnupf, U.; Bosma, W. B. *Carbohydr. Res.* **2006**, *341*, 525–537.
24. Scholzová, E.; Mach, P.; Hricovíni, M. *Molecules* **2003**, *8*, 770–779.
25. Remko, M.; Hricovíni, M. *Struct. Chem*., in press.
26. JAGUAR 3.5, Schrodinger, Inc., Portland, 1998.
27. Parr, R. G.; Wang, W. *Density-Functional Theory of Atoms and Molecules*; Oxford University Press: New York, 1994.
28. Lee, C.; Yang, W.; Paar, R. G. *Phys. Rev. B* **1988**, *37*, 785–789.
29. Becke, A. D. *J. Chem. Phys.* **1993**, *98*, 5648–5652.
30. Becke, A. D. *Phys. Rev. A* **1988**, *38*, 3098–3100.
31. Vosko, S. H.; Wilk, L.; Nusair, M. *Can. J. Phys.* **1980**, *58*, 1200–1208.
32. Frisch, M. J.; Trucks, G. W.; Schlegel, H. B.; Scuseria, G. E.; Robb, M. A.; Cheeseman, J. R.; Montgomery, J. A., Jr.; Vreven, T.; Kudin, K. N.; Burant, J. C.; Millam, J. M.; Iyengar, S. S.; Tomasi, J.; Barone, V.; Mennucci, B.; Cossi, M.; Scalmani, G.; Rega, N.; Petersson, G. A.; Nakatsuji, H.; Hada, M.; Ehara, M.; Toyota, K.; Fukuda, R.; Hasegawa, J.; Ishida, M.; Nakajima, T.; Honda, Y.; Kitao, O.; Nakai, H.; Klene, M.; Li, X.; Knox, J. E.; Hratchian, H. P.; Cross, J. B.; Bakken, V.; Adamo, C.; Jaramillo, J.; Gomperts, R.; Stratmann, R. E.; Yazyev, O.; Austin, A. J.; Cammi, R.; Pomelli, C.; Ochterski, J. W.; Ayala, P. Y.; Morokuma, K.; Voth, G. A.; Salvador, P.; Dannenberg, J. J.; Zakrzewski, V. G.; Dapprich, S.; Daniels, A. D.; Strain, M. C.; Farkas, O.; Malick, D. K.; Rabuck, A. D.; Raghavachari, K.; Foresman, J. B.; Ortiz, J. V.; Cui, Q.; Baboul, A. G.; Clifford, S.; Cioslowski, J.; Stefanov, B. B.; Liu, G.; Liashenko, A.; Piskorz, P.; Komaromi, I.; Martin, R. L.; Fox, D. J.; Keith, T.; Al-Laham, M. A.; Peng, C. Y.; Nanayakkara, A.; Challacombe, M.; Gill, P. M. W.; Johnson, B.; Chen, W.; Wong, M. W.; Gonzalez, C.; Pople, J. A. GAUSSIAN03, *Revision C.02*; Gaussian: Wallingford, CT, 2004.
33. Godbout, N.; Salahub, D. R.; Andzelm, J. E.; Wimmer, E. *Can. J. Chem.* **1992**, *70*, 560–571.
34. Tannor, D. J.; Marten, B.; Murphy, R.; Friesner, R. A.; Sitkoff, D.; Nicholls, A.; Ringnalda, M.; Goddard, W. A.; Honig, B. *J. Am. Chem. Soc.* **1994**, *116*, 11875–11882.
35. Barone, V.; Cossi, M.; Tomasi, J. *J. Comput. Chem.* **1998**, *19*, 404–417.
36. Whitfield, D. M.; Birnbaum, G. I.; Pang, H.; Baptista, J.; Sarkar, B. *J. Carbohydr. Chem.* **1991**, *10*, 329–348.
37. Yates, E. A.; Mackie, W.; Lamba, D. *Int. J. Biol. Macromol.* **1995**, *17*, 219–223.
38. Lamba, D.; Mackie, W.; Rashid, A.; Sheldrick, B.; Yates, E. A. *Carbohydr. Res.* **1993**, *241*, 89–98.
39. Haasnoot, C. A. G.; DeLeeuw, F. A. A. M.; Altona, C. *Tetrahedron* **1980**, *36*, 2783–2792.
40. Hricovíni, M.; Malkina, O. L.; Bízik, F.; Turi-Nagy, L.; Malkin, V. G. *J. Phys. Chem. A* **1997**, *101*, 9756–9762.